

UPRATED OMS ENGINE STATUS - SEA LEVEL TESTING RESULTS

14737

J. D. Bertolino
Aerojet Propulsion Division
Sacramento, California

AE 604394

W. C. Boyd
NASA Johnson Space Center
Houston, Texas
PRA-SA-NASA Johnson

ND 185000

ABSTRACT

The current Space Shuttle Orbital Maneuvering Engine (OME) is pressure fed, utilizing storable propellants. Performance uprating of this engine, through the use of a gas generator driven turbopump to increase operating pressure, is being pursued by the NASA Lyndon B. Johnson Space Center (JSC). Component level design, fabrication, and test activities for this engine system have been on-going since 1984. More recently, a complete engine, designated the Integrated Component Test Bed (ICTB), has been tested at sea level conditions by Aerojet. A description of the test hardware and results of the sea level test program are presented. These results, which include the test condition operating envelope and projected performance at altitude conditions, confirm the capability of the selected Uprated OME (UOME) configuration to meet or exceed performance and operational requirements. Engine flexibility, demonstrated through testing at two different operational mixture ratios, along with a summary of projected Space Shuttle performance enhancements using the UOME, are discussed. Planned future activities, including ICTB tests at simulated altitude conditions, and recommendations for further engine development, are also discussed.

INTRODUCTION

The Orbital Maneuvering System (OMS) is the Space Shuttle Orbiter's primary propulsion system for on-orbit operations. The OMS, shown in Fig. 1, provides the necessary thrust for the Orbiter to perform final orbit insertion, orbit circularization, orbital transfer maneuvers, rendezvous maneuvers, deorbit, and abort maneuvers. Central to this system is the OME. The 26.7 kN (6,000 lbf) thrust pressure-fed OME operates at a chamber pressure (P_c) of 8.6 bar (125 psia) and a mixture ratio (MR) of 1.65:1. It uses monomethylhydrazine (MMH) fuel to regeneratively cool the combustion chamber where it reacts with the nitrogen tetroxide (NTO) oxidizer. The engine, as depicted in Fig. 1, has a nozzle expansion ratio of 55:1 and provides a specific impulse (Isp) of 315 seconds.

The use of a pressure fed operating cycle results in a very simple and reliable OME. However, a pressure fed cycle requires a fairly high propellant tank pressure [17.2 bar (250 psia) for the OMS], and does not take full advantage of more sophisticated operating cycles.

The Aerojet Propulsion Division is under contract to JSC to demonstrate the feasibility of uprating the OME performance by adding a gas generator driven turbopump assembly to increase propellant pressure at the chamber inlet. Uprating this engine by increasing chamber pressure to 24.1 bar (350 psia) allows a smaller throat, and thus a greater expansion ratio within the same envelope and thrust level. In addition, the injector pattern has been modified to provide an energy release efficiency (ERE) of 99% when operated at a mixture ratio of 1.95:1. The net effect of these changes is an increase in OME Isp of 19 seconds to 334 seconds.

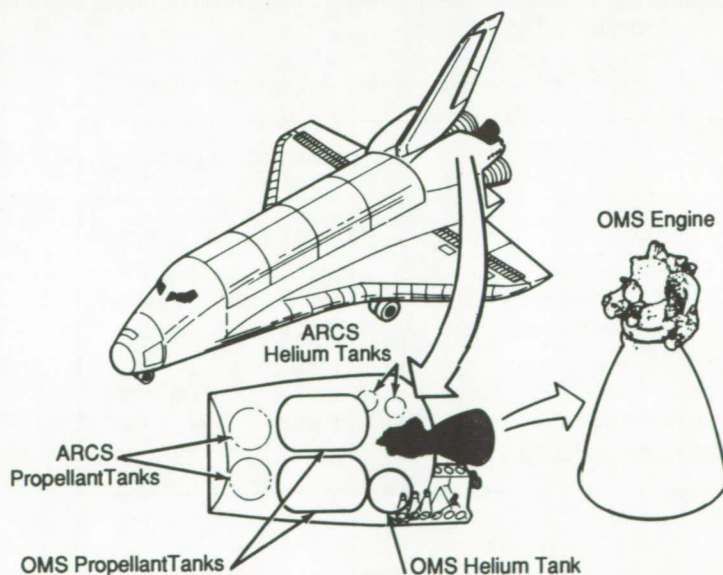


Fig. 1. Space Shuttle Orbital Maneuvering System

Approved for public release; distribution is unlimited.

UPRATED OME APPLICATION

The most obvious benefit derived from use of the UOME would be increased payload capability for the Space Shuttle. For a UOME with 334 second Isp, the decrease in required propellant to impart a 305 m/sec (1,000 ft/sec) delta velocity to an orbiter initially weighing 115,214 kg (254,000 lbm), is 590 kg (1,300 lbm) which translates directly to an increase in allowable Orbiter dry weight, including payload, of 590 kg (1,300 lbm). This results solely from the retro-fit of the engine into existing pods. With accompanying pod modifications, such as light weight propellant tanks and the reduction in pressurization system mass, payload gains in the 1361 kg (3,000 lbm) range could be attained.

If the increased performance offered by the UOME is used to increase delta velocity, the maximum attainable orbit can be increased by 10 to 20 nautical miles. For specific payload applications, this increased orbit capability can extend the time in orbit before payload reboost is required.

In addition, the need for a high performance upper stage that can place payloads in Geostationary Earth Orbit (GEO) or on planetary missions continues to grow. The termination of efforts to integrate the cryogenic Centaur stage into the Orbiter means there is currently no stage being developed for use on the Orbiter that can deliver the very heavy payloads [over 2268 kg (5,000 lbm)] to GEO. Existing STS-compatible stages are all solid fueled (PAM and IUS), with relatively low payload weight capability.

The UOME also has application for delivery of payloads on interplanetary trajectories due to the engines restart capability, and the use of storable propellants provides unlimited in-space stay time. An example is the Mars sample return mission.

While performance improvement is the primary objective of the UOME engine program, an equally important objective has been to minimize the impact to the Orbiter and all aspects of flight operation. Key to minimizing orbiter impacts was maintaining the current engine redundancy, contingency operation, envelope, and cycle life capability. While these necessary attributes may constrain the design of the engine, it is felt that an upper stage application of this engine would benefit from the enhanced reliability, and with the synergy that results from commonality with the OMS.

UPRATED OME DESCRIPTION

OVERVIEW

Table I summarizes the general operating characteristics for the UOME as compared to the current Space Shuttle OME. The UOME is shown in Fig. 2, and depicted schematically in Fig. 3.

Table I. Characteristics of the OME and the UOME

	CURRENT OME	UPRATED OME
THRUST, kN (lbf)	26.7 (6,000)	26.7 (6,000)
CHAMBER PRESSURE, bar (psia)	8.6 (125)	24.1 (350)
NOZZLE EXPANSION RATIO	55:1	155:1
DRY WEIGHT, kg (lbm)	135 (297)	146 (322)
CYCLE LIFE	125	125
		500 (goal)
MIXTURE RATIO	1.65:1	1.95:1/1.65:1
SPECIFIC IMPULSE, sec	314	334/331

ORIGINAL PAGE BLACK AND WHITE PHOTOGRAPH

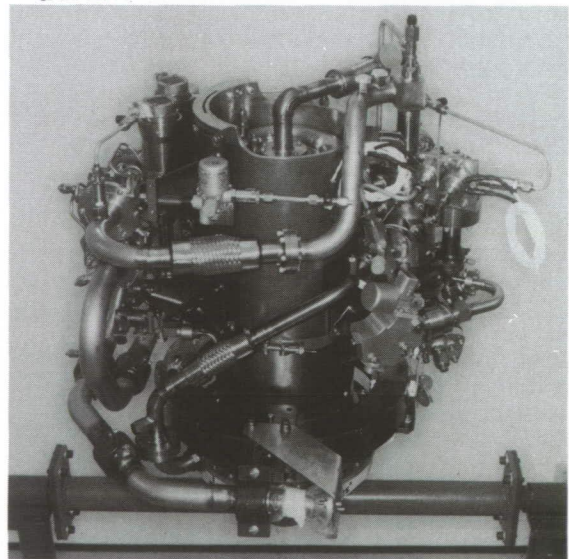


Fig. 2. UOMS Engine

Propellants supplied to the engine inlets are flow controlled by the bipropellant valve located upstream of the turbopump assembly, which provides the pressure increase necessary to operate the engine at its uprated chamber pressure of 24.1 bar (350 psia). Fuel entering at the chamber aft flange travels up through the coolant channels and is injected into the main chamber where it combusts with the oxidizer. Propellant tap-offs

downstream of the turbopump supply the gas generator which, in turn, supplies the turbine drive gas. After driving the turbine, the exhaust gases are ducted to a nozzle coolant manifold which supersonically injects the gas into the nozzle for cooling, and to enhance engine performance (versus an overboard dump).

Engine operation is initiated by opening the turbine start and bipropellant valves. Gaseous helium is provided by the turbine start system, which initiates turbopump rotation. When pump discharge pressure rises above the start system pressure, the gas generator valves are opened and the turbine start valve is closed. Combustion in the gas generator then provides the necessary turbine drive gas to bootstrap the engine to its operating chamber pressure.

Engine shutdown is accomplished by closing of the gas generator and bipropellant valves. Gaseous helium purges are then initiated to expel propellants from the fuel and oxidizer circuits downstream of the bipropellant valve.

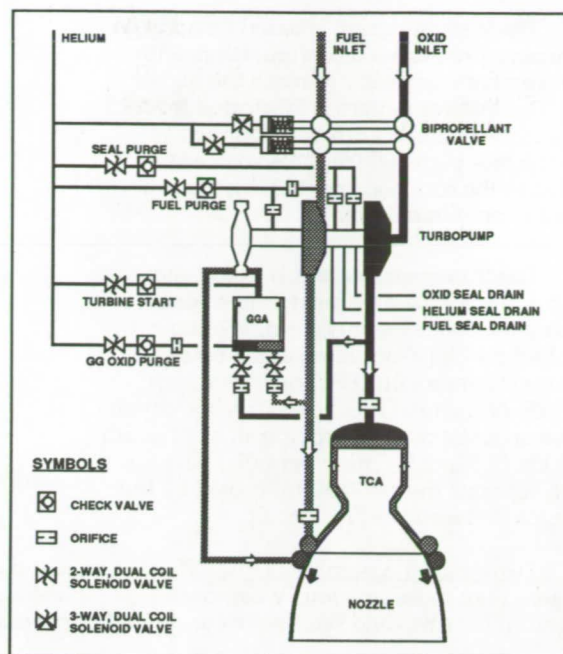


Fig. 3. UOMS Engine System Schematic

COMPONENT DESCRIPTIONS

Thrust Chamber Assembly (TCA). The UOME thrust chamber, which is a derivative of the current OME chamber, is a single pass, regeneratively cooled assembly. A cross section of the chamber is shown in Fig. 4. The coolant (fuel) enters the chamber through the aft fuel torus and flows up to the injector through 104 slots milled in the chamber liner wall, which are closed out with electroformed nickel. The injector is electron beam welded to the forward end of the chamber (internal weld) and to the CRES 304 closeout ring (external weld) to form the assembly.

The chamber diameter of 14 cm (5.5 inches) is 6.6 cm (2.6 inches) less than the current design. The 35.6 cm (14 inch) chamber length, based upon injector test results, was required to attain a 99% ERE. The divergent section of the chamber has a half angle of 33 degrees, and the exit area ratio is 6:1. Thrust chamber assembly design and operating characteristics are summarized in Table II.

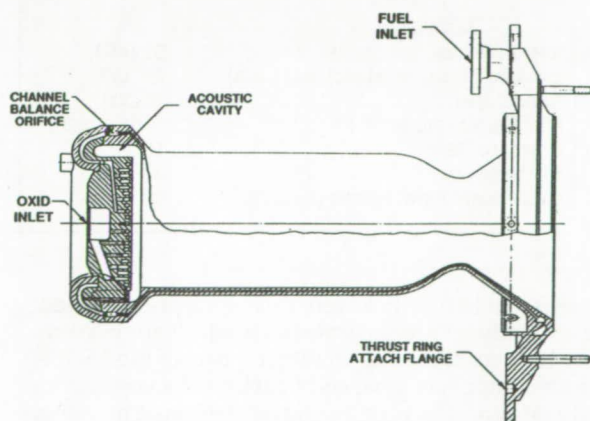


Fig. 4. Thrust Chamber Assembly

Table II. Thrust Chamber Assembly Design And Operating Characteristics

PARAMETER	VALUE
Nominal Chamber Diameter, cm (in.)	14 (5.5)
Throat Diameter, cm (in.)	8.5 (3.36)
Exit Area Ratio	6:1
Contraction Ratio	2.70
Chamber Length (L'), cm (in.)	35.6 (14)
Fuel Flow Rate, kg/sec (lb/sec)	2.6 (5.8)
Oxidizer Flow Rate, kg/sec (lb/sec)	5.3 (11.7)
Chamber Pressure (Pc), bar (psia)	24.1 (350)
Fuel Inlet Pressure, bar (psia)	53.1 (770)
Oxidizer Inlet Pressure, bar (psia)	39.6 (575)
Injector Fuel Temperature (Tf), °K (°F)	416 (290)
Mixture Ratio	2.0

A key engine design issue is the selection of a chamber material that will give the required cycle life. The higher throat heat flux due to increased chamber pressure results in hot gas wall temperatures that severely impact cycle life. The life of the current CRES 304L liner material would be reduced from its current value of 125 usable cycles to only 25 at the uprated chamber pressure of 24.1 bar (350 psia). Nickel 201, selected as the chamber liner material due to its greater conductivity over 304L, provides a cycle life which exceeds 500 cycles.

The injector design is based heavily on the current pressure-fed configuration, with improvements necessary to reach the higher ERE. The injector pattern is fabricated from 15 photo etched platelets diffusion bonded to form the face plate, which is electron beam welded to the core body containing the propellant supply manifolds.

The transverse platelet injector, shown in Fig. 5, has a mixed element pattern using 378 splash plate core elements, a single outer row of 72 like-on-like X-doublets, and a boundary of 36 fuel film coolant (FFC) orifices which inject 4% of the total fuel flow. Twelve equally spaced acoustic cavities provide an axial depth of 0.8 cm (0.3 inch). Circumferential partitions, which separate the cavities, are cooled by fuel passages that feed the FFC circuit.

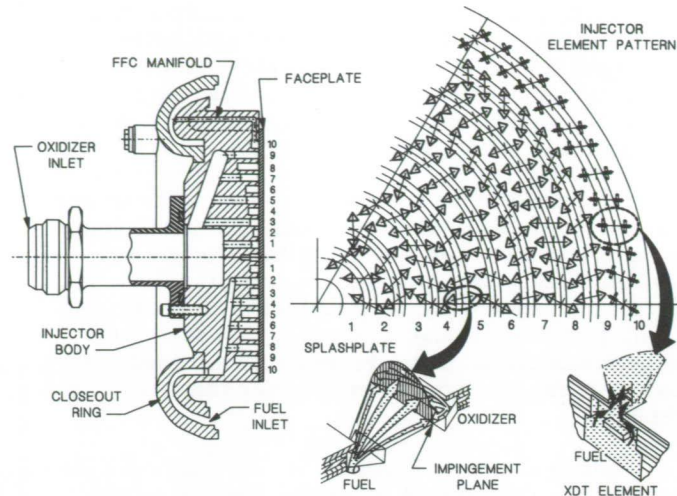


Fig. 5. Detail of Injector Assembly and Faceplate

Turbopump Assembly (TPA). The duration and cycle life requirements of the UOME are significantly more stringent than those previously demonstrated for a storable propellant turbopump assembly. Turbine rotor blades, and pump bearings and seals were considered important components in attaining high cycle life.

The turbopump assembly consists of fuel and oxidizer centrifugal pumps driven by an outboard turbine, all on a common shaft. This configuration simplifies the design and separates the higher temperature turbine from the cooler pump cavities. A cross section of the turbopump assembly is shown in Fig. 6, and the design and operating characteristics are provided in Table III.

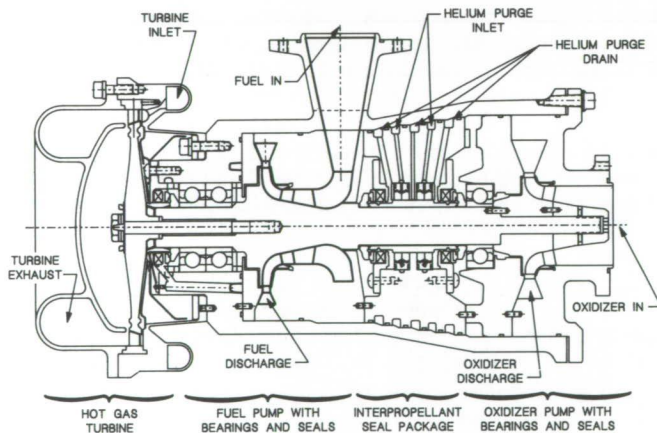


Fig. 6. Turbopump Assembly

Table III. Turbopump Assembly Design And Operating Characteristics

PUMP	FUEL	OXID
Weight Flow, kg/sec (lb/sec)	2.8 (6.14)	5.4 (11.82)
Inlet Pressure, bar (psia)	4.7 (68)	6.3 (92)
Inlet Temperature, °K (°F)	294 (70)	294 (70)
Discharge Pressure, bar (psia)	63.8 (925)	47.3 (686)
Speed, rpm	40K	40K
Efficiency, %	66	73
Shaft Power, kW (SHP)	28.6 (38.4)	21.1 (28.3)
Tare Power, kW (SHP)	10.4 (13.9)	
TURBINE		
Inlet Pressure, bar (psia)	31 (450)	
Exhaust Pressure (static), bar (psia)	2.1 (30)	
Speed, rpm	40,000	
Inlet Temperature, °K (°F)	1155 (1,620)	
Pressure Ratio	15.1	
Efficiency, %	37	
Gas Weight Flow, kg/sec (lb/sec)	0.15 (0.34)	

The single stage, dual partial admission Waspalloy turbine is mechanically keyed, through a pretensioned coupling, to the turbopump shaft. The oxidizer pump impeller and inducer are separate parts which are piloted and pinned to the shaft. The fuel pump impeller and inducer are both machined as an integral part of the 15-5PH stainless steel shaft. Each inducer has four blades, and the shrouded impellers have eight backward swept blades. The pump discharge housings are single volute, constant velocity design. The turbine inlet and exhaust manifolds are made of Haynes 188.

The turbine end bearing package consists of a 1.7 cm (0.67 inch) duplex ball bearing set that reacts thrust loads in both directions and radial loads. The oxidizer end bearing is a 1.5 cm (0.59 inch) ball bearing for radial support only. The bearings are cooled by propellants, which flow from the pump discharges through metered labyrinths. The propellant coolant flows provide some lubrication, but the primary lubrication comes from the Teflon impregnated cages.

The reliability of the turbopump assembly is significantly impacted by the ability to isolate the propellants from each other under both nominal and failure situations. Both the turbine and pump shaft seals are rubbing contact face type seals with secondary nested ripple bellows seals. The primary dynamic seals are carbon/graphite nosepieces which mate with running rings. In addition, four sets of spring loaded graphite shaft seals further isolate the two propellants. A continuous helium purge is supplied to these seals to provide a positive inert pressure to the interpropellant cavity. The design of the interpropellant seal package assures that no single seal element failure results in propellant mixing. With adequate instrumentation, any seal failure can be detected, and safe shutdown achieved.

Gas Generator (GG). A fuel rich gas generator is used in the UOME to provide heated gas with sufficient energy to drive the turbopump assembly. The gas generator burns the same propellants as the main thrust chamber, utilizing approximately 2% of the total propellant flow. Figure 7 shows the gas generator assembly.

The Haynes-188 cylindrical chamber has a 1.9 cm (0.75 inch) ID and is 10.2 cm (4 inches) long. It incorporates a 1.4 cm (0.56 inch) ID turbulence ring 4.6 cm (1.8 inches) from the injector face to mix the combustion gases and provide a uniform turbine inlet gas temperature. The injector design is based on the X-doublet pattern, and contains 48 fuel elements surrounding six oxidizer elements. The injector is fabricated from 63 photo etched platelets, diffusion bonded to form the assembly. Gas generator design and operating characteristics are provided in Table IV.

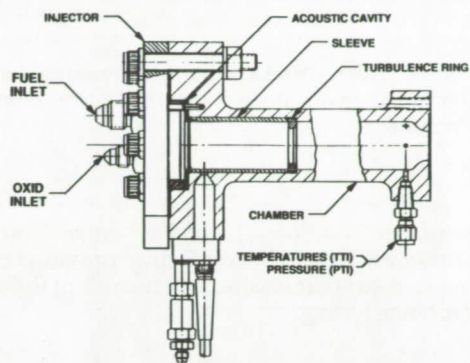


Fig. 7. Gas Generator Assembly

Table IV. Gas Generator Design And Operating Characteristics

PARAMETER	VALUE
Chamber Pressure (PcGG), bar (psia)	32.8 (475)
Exhaust Gas Temperature, °K (°F)	1155 (1,620)
Temperature Uniformity, °K (°F)	±55 (±100)
Mixture Ratio	0.18
Fuel Flow Rate, kg/sec (lb/sec)	0.13 (0.28)
Oxid Flow Rate, kg/sec (lb/sec)	0.02 (0.05)
Fuel Inlet Pressure*, bar (psia)	48.3 (700)
Oxid Inlet Pressure*, bar (psia)	43.1 (625)

* values upstream of GG control valves

Control Components. The bipropellant valve is identical to the current OME valve and is used without modification. The valve assembly is actually two series redundant bipropellant valves. Helium actuation pressure for each bipropellant valve is controlled by three-way, dual coil solenoid valves. The actuation pressure acts on a piston, which moves an integral rack gear linearly. The rack gear, in turn, rotates pinion gears attached to each of two ball valves (one for each propellant), which provide the on-off flow control. Coil springs in the actuator cavity provide the closing force when the helium pressure is removed.

The gas generator valves are dual coil coaxial, bipolar designs with flat faced armatures. The Teflon seal is integrated into the armature, which is Belleville spring loaded to provide the closing force. Disc type 100 micron (absolute) filters are included in the valve inlets to prevent seal contamination.

The turbine start circuit routes helium gas to the turbine to initiate turbopump rotation and bootstrap start. The Turbine Start Valve is a solenoid piloted, two-way, normally closed valve utilizing inlet pressure for operation. The Turbine Start Check Valve is a spring/pressure operated, in-line valve which allows helium flow in one direction and prevents gas generator products from entering the helium system.

The Helium Purge Valves are normally closed, two-way, two position solenoid actuated valves. In-line check valves are used to isolate the purge system from the propellant circuits.

Integrating Components. Components from the current OME which are used unmodified on the UOME include the thrust mount and gimbal ring, propellant inlet feedlines and bellows, the bipropellant valve, and bipropellant valve mounting bracket.

New propellant feedlines for pump suction and discharge are required, along with turbopump and control component mounting brackets. A cylindrical shell assembly, which surrounds the thrust chamber and bolts to the aft flange is used for component mounting.

ICTB SEA LEVEL TEST PROGRAM

After completing a series of design, fabrication, and test efforts on the critical engine components, the next logical step in demonstrating the capabilities of the UOME engine was to assemble these components into an Integrated Components Test Bed (ICTB) to demonstrate the performance and operational goals of a complete engine system. As a pre-development activity, the ICTB provides a sound experience base in areas such as fabrication, engine system analysis, and engine operating issues. Specific areas to be addressed included definition of engine/system interactions and interface issues, determination of component interfaces, and characterization of engine performance.

TEST OBJECTIVES

The primary objective of the ICTB test program was to demonstrate sea level operation of the pump fed engine assembly. Issues that were resolved for the ICTB assembly included the start-up and shutdown sequencing of the engine, the effect of thermal soakback on critical components, the impact of off-design inlet conditions, and thrust tail-off characteristics.

The ICTB assembly was tested at two different mixture ratios to demonstrate operational flexibility. The current ICTB engine system was designed to operate at a 1.95:1 mixture ratio to maximize engine performance. To demonstrate system compatibility with the existing OMS, the ICTB engine was also tested at 1.65:1 engine mixture ratio. These two different mixture ratios resulted in two different ICTB system balance points, but did not require different start-up/shutdown sequencing.

In addition, the testing provided data on component interactions, which could not be fully evaluated at the component level. This includes volume fill times, back pressure effects, thermal transients, control component response times, and the engine induced vibration and acoustic environment.

TEST FACILITY

The ICTB engine test series was conducted at sea level conditions on Test Stand J-4 of the Aerojet Propulsion Division J-Area test facility. All testing was done in the horizontal firing attitude. The test facility provided engine control (sequencer), data recording instrumentation, and all the attendant support equipment, including fluid and electrical supply. This same test stand is used for current OME acceptance testing.

TEST PLAN AND APPROACH

As the testing was performed at sea level conditions, the assembly did not include the components necessary for altitude operation (nozzle coolant manifold, turbine exhaust line, and nozzle extension). Turbine exhaust gases (gas generator combustion products) were ducted overboard through a separate conduit. This duct was configured so that exhaust products did not contribute to or detract from the measured thrust.

The analytical methods used to control system parameters included: (1) the Liquid Engine Equilibrium Simulation (LEES) program - a steady state model of the storable gas generator cycle engine used to define orifice sizes required to have the engine run at the desired operating points, and (2) the Liquid Engine Transient Simulation (LETS) program - a library of fluid dynamic/thermodynamic elements used to create a transient model of the gas generator engine. Simulations were run with the LETS model in order to define valve sequencing used in testing to accomplish a successful bootstrap start. Model accuracy was checked by comparing predictions with test data.

Engine chamber pressure and mixture ratio balance was achieved using in-line orifices installed in both the fuel and oxidizer propellant circuits, at the thrust chamber assembly inlets and gas generator injector.

The ICTB engine sea level test program consisted of the five following test series.

Test Series I - The initial eight tests were conducted to obtain balance and sequencing for ICTB engine operation at a 1.95 mixture ratio. The first three tests were required to establish the helium start system parameters. The gas generator valves were not opened until the sixth test, which was the first full system checkout. Data from this test was used to converge on a system balance.

Test Series II - After engine balance and sequencing were established in Series I, six tests were conducted to investigate steady state performance at the 1.95 mixture ratio operating point.

Test Series III - Four tests were conducted to define the balance and sequencing for engine operation at a 1.65 mixture ratio.

Test Series IV - After engine balance was established in series III, steady state performance at a 1.65 mixture ratio was investigated. Three tests were conducted to obtain engine system thermal steady state, and investigate any performance shifts during a long duration (160 second) burn.

Test Series V - Five tests were conducted in this series to investigate the effect of varying propellant inlet pressures on engine system balance and performance.

TEST RESULTS

Test Summary. The ICTB sea level test program consisted of 26 tests with a total firing duration of 694 seconds. A summary of the tests run at 1.95 mixture ratio is provided in Table V. A summary of the 1.65 mixture ratio tests is provided in Table VI. A typical test firing is shown in Fig. 8.

Table V. 1.95 Mixture Ratio Test Summary

Test Series	Test No.	Dur. (sec)	M.R.	Pc bar (psia)	Flow kg/s(lb/s)	Speed (rpm)	PcGG bar (psia)	TTI K(°F)
I	001	2.1	1.97	16.3 (236)	5.30 (11.68)	—	15.4 (224)	N/A
I	002	2.1	1.95	17.0 (247)	5.56 (12.25)	28,348	16.8 (244)	N/A
I	003	2.1	1.96	16.8 (244)	5.49 (12.10)	28,267	16.4 (238)	N/A
I	004	0.7						
I	005	0.5						
Inadequate Duration for Data								
I	006	8.1	1.87	25.5 (370)	8.41 (18.54)	41,813	35.2 (511)	1129 (1573)
I	007	15.1	1.92	25.6 (371)	8.45 (18.63)	42,203	35.7 (518)	1143 (1598)
I	008	15.1	1.93	24.3 (352)	8.01 (17.66)	40,119	32.3 (468)	1111 (1541)
II	009	4.9	1.94	24.1 (349)	7.96 (17.55)	42,204	32.1 (465)	1149 (1609)
II	010	13.5	1.96	24.8 (360)	8.20 (18.07)	41,113	33.4 (484)	1166 (1640)
II	011	30.1	1.95	24.5 (355)	8.08 (17.82)	40,371	33.0 (478)	1170 (1646)
II	012	25.5	1.95	24.3 (353)	8.03 (17.70)	40,618	32.8 (476)	1169 (1644)
II	013	34.5	1.93	24.7 (358)	8.15 (17.96)	41,079	33.4 (485)	1167 (1641)
II	014	80.1	1.94	23.9 (347)	7.91 (17.44)	39,790	31.6 (459)	1086 (1494)

NOTE: Tests 001 Thru 005 Turbine Cold Gas Flow Only

Table VI. 1.65 Mixture Ratio Test Summary

Test Series	Test No.	Dur. (sec)	M.R.	Pc bar (psia)	Flow kg/s(lb/s)	Speed (rpm)	PcGG bar (psia)	TTI K(°F)
III	015	2.1	1.85	16.5 (240)	5.39 (11.89)	28,066	N/A	N/A
III	016	15.1	1.69	25.3 (367)	8.33 (18.36)	41,123	34.8 (505)	1036 (1399)
III	017	15.1	1.67	25.1 (364)	8.26 (18.20)	39,639	34.3 (497)	1155 (1620)
III	018	15.1	1.68	25.0 (362)	8.20 (18.08)	40,825	34.0 (493)	1149 (1608)
IV	019	30.1	1.68	24.9 (361)	8.21 (18.09)	40,559	34.1 (495)	1156 (1622)
IV	020	160.0	1.68	24.6 (357)	8.11 (17.88)	40,610	34.0 (493)	1159 (1627)
IV	021	160.0	1.68	24.5 (355)	8.05 (17.75)	40,225	33.8 (490)	1154 (1617)
V	022	1.5						
Inadequate Duration for Data								
V	023	15.1	1.72	24.5 (355)	8.04 (17.73)	40,629	33.5 (486)	1179 (1662)
V	024	15.1	1.64	25.3 (367)	8.28 (18.26)	41,394	34.9 (506)	1145 (1599)
V	025	15.1	1.63	24.7 (358)	8.11 (17.87)	41,014	34.0 (493)	1135 (1584)
V	026	15.1	1.71	23.9 (347)	7.87 (17.34)	40,287	32.5 (471)	1171 (1649)

Start And Shutdown Transients. After opening of the bipropellant and turbine start valves, turbopump rotation was initiated. Approximately 0.9 seconds after Fire Switch 1 (FS-1), combustion in the main chamber reached a steady 16.5 bar (240 psia) with no combustion instability or pump speed overshoot. The gas generator valves were opened 1.5 seconds after FS-1 (with a 0.1 second fuel valve lead to assure no transient turbine temperature spikes occurred), and the engine bootstrapped smoothly to its operating pressure of 24.1 bar (350 psia) Pc and turbopump speed of 40,000 rpm. Full power was achieved approximately 4 seconds after FS-1. A typical start transient is shown in Fig. 9.

Shutdown was accomplished by closing the gas generator and bipropellant valves. A gas generator fuel valve lag of 0.1 seconds assured no turbine temperature spikes occurred. Shutdown to zero thrust was achieved approximately 0.5 seconds after Fire Switch 2 (FS-2). Purges were then initiated to expel propellants from the fuel and oxidizer circuits downstream of the bipropellant valve. A typical shutdown transient is shown in Fig. 10.

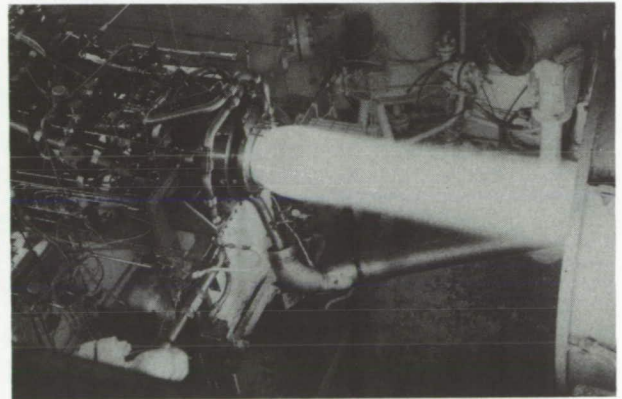


Fig. 8. UOME ICTB Test Firing (Typical)

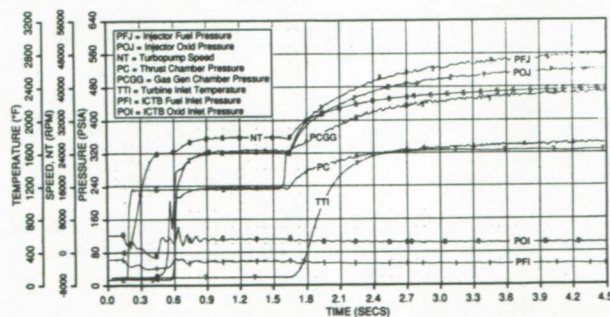


Fig. 9. UOME ICTB Start Transient (Typical)

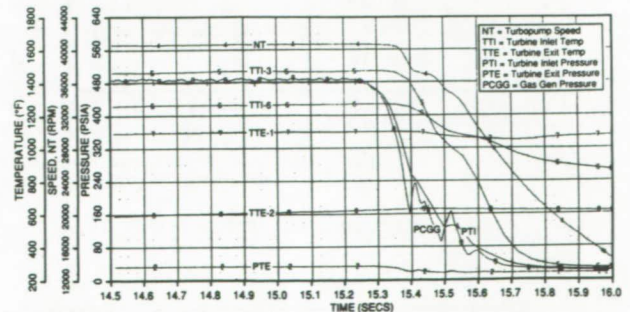


Fig. 10. UOME ICTB Shutdown Transient (Typical)

Engine Performance. The performance data from ICTB engine testing was correlated against the operating variables of chamber pressure (P_c), mixture ratio (MR), and injector fuel temperature (T_{fj}), using a multiple covariance program. A multiple covariance analysis was then made of the I_{sp} , thrust coefficient (C_f), and characteristic exhaust velocity (C^*).

In a flight configuration engine, specific impulse penalty is paid for the small percentage of the engine flow rate that is diverted to the gas generator and burned to generate the hot gas needed to run the turbopump. The specific impulse produced by injecting these GG products into the nozzle is significantly less than that produced by the main injector flow. Total engine I_{sp} is calculated as the mass weighted sum of the injector flow I_{sp} and the GG gas product I_{sp} .

During ICTB engine testing, total propellant weight flow and GG fuel flow (which can be used to estimate total GG flow) were measured. TCA thrust only was measured, as the GG gas products were ducted overboard through a separate non thrust measuring conduit. Without knowledge of GG thrust, it is only possible to directly determine TCA I_{sp} .

The difference between the injector flow I_{sp} (TCA I_{sp}) and the overall engine I_{sp} is designated as the gas generator performance loss. Since only the overall thrust generated by the engine was measured, the gas generator product I_{sp} could not be independently determined. Therefore, the performance loss was derived from a calculated one-dimensional frozen flow expansion of the gases over the design pressure ratio from the nozzle coolant manifold injection pressure to the nozzle exit pressure. The nominal predicted gas generator performance loss is 3.3 seconds.

A plot of predicted I_{sp} versus mixture ratio for engine altitude performance (including the predicted gas generator performance loss) using the standard two-dimensional kinetic (TDK) computer program extrapolated to $A_e/A_t = 162:1$, normalized to $P_c = 24.1$ bar (350 psia), $T_{fj} = 422^\circ\text{K}$ (300°F), is shown in Fig. 11.

TCA Performance. The thrust chamber assembly (TCA) operation throughout the test program was excellent. There was no indication of combustion instabilities, pressure perturbations or other anomalies. A post test inspection showed no signs of streaking, cracking, leakage or other damage.

The injector performance was comparable with the previous injector test history of 99% ERE. A plot of energy release efficiency (ERE) versus TCA mixture ratio and chamber pressure is provided in Fig. 12.

The chamber fuel coolant bulk temperature rise versus engine mixture ratio and firing duration is provided in Fig. 13. Over the mixture ratio range tested, a 25.6°K (46°F) increase from $MR = 1.6$ to 2.0 was observed. The fuel bulk temperature rise rate across the chamber indicates that chamber steady state thermal conditions occur 60 to 80 seconds after start, depending on individual test conditions.

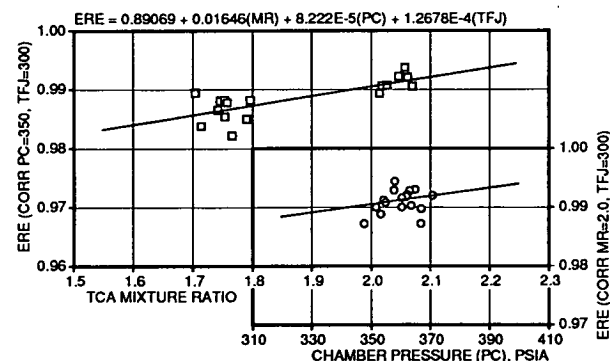


Fig. 12. Injector ERE Versus MR and P_c

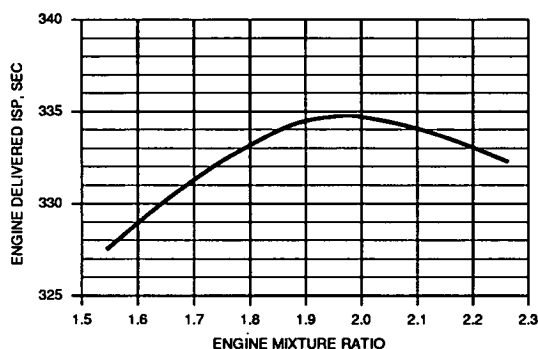


Fig. 11. Predicted Altitude I_{sp} Versus Mixture Ratio

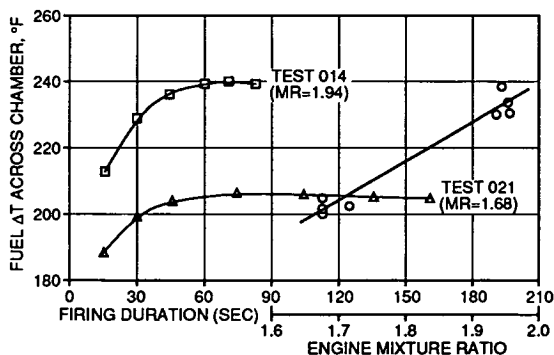


Fig. 13. Fuel Coolant Bulk Temperature Rise Rate Versus Mixture Ratio and Firing Duration

Turbopump Assembly Performance. Bearing and seal performance during the test series was flawless. Bearing temperatures were within the specified limits during both operation and soak back. There was no change in the interpropellant seal purge and drain pressures and there was no evidence of bellows seal leakage.

The noncavitating pump performance is represented by head (H/N^2) and flow (Q/N) coefficients. The volumetric flow rate (Q) was directly measured with flow meters installed in the engine inlet lines. The pump head rise (H) is calculated from the total pressure difference between pump suction and discharge. The total pressure is the summation of the measured static pressure and local kinetic pressure (velocity head) calculated from the volumetric flow rate and pipe area. The pump efficiency was not directly measured. In order to separate the turbine and pump efficiencies from the total TPA efficiency, the predicted pump efficiency was used to calculate the pump horsepower. Figures 14 and 15 show the fuel and oxidizer pump performances for the sea level test program.

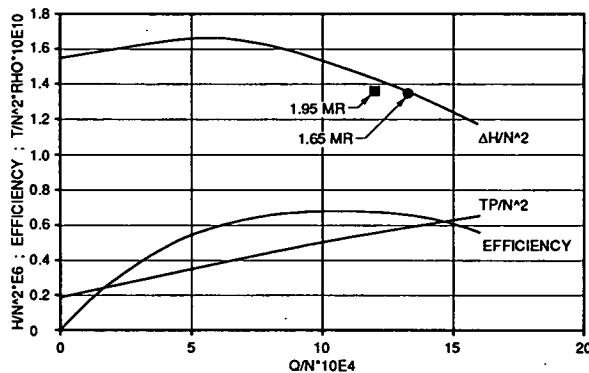


Fig. 14. Fuel Pump Performance

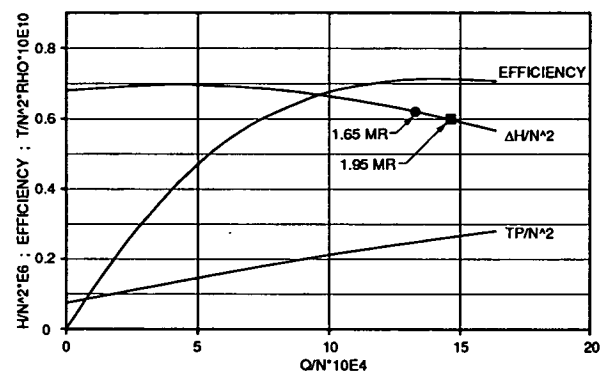


Fig. 15. Oxidizer Pump Performance

Turbine shaft horsepower was determined as the sum of required pump horsepower and estimated TPA tare horsepower. Turbine pressure ratio and subsequent calculations were based on turbine manifold entrance pressure (PTI) to turbine manifold exit pressure (PTE). The turbine flow rate, used to determine turbine performance, was based on an equivalent nozzle C_dA , turbine inlet temperature and pressure, and gas properties. Turbine performance for the sea level test program is shown in Fig. 16.

Variable Propellant Inlet Pressure Survey. During Test Series V, the maximum effect experienced in MR was 1.63 to 1.72 and in P_c was 23.9 to 25.3 bar (347 to 367 psia). The effect of varying inlet pressures is shown in Fig. 17.

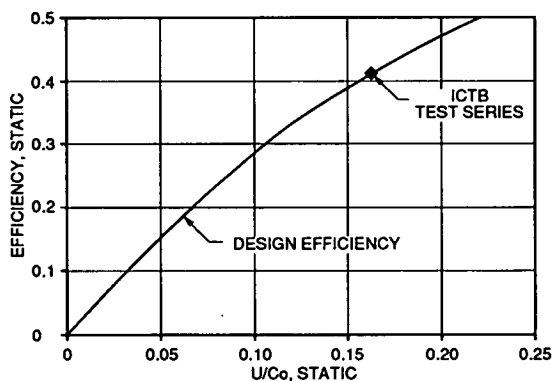


Fig. 16. Turbine Performance

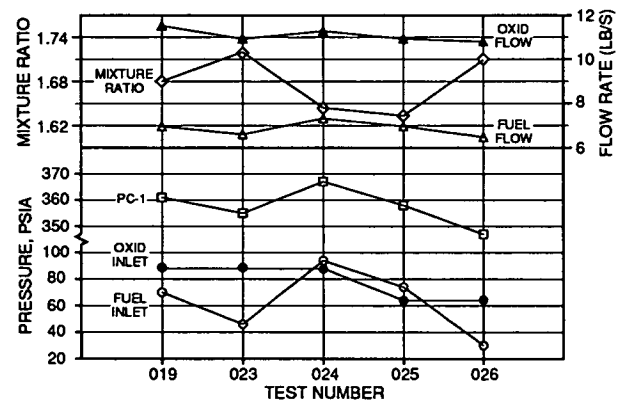


Fig. 17. Effect of Varying Inlet Pressures

SUMMARY AND CONCLUSIONS

The UOME ICTB sea level test program was extremely successful. Major accomplishments included demonstration of start and shutdown transients, operation at both 1.95 and 1.65 engine mixture ratios with balance orifice changes only, and operation at varied inlet pressures. The design performance goal of 99% injector ERE was met, with no evidence of component degradation or damage. Combustion stability was demonstrated over a wide range of operating conditions, and the engine had a high degree of bootstrap margin.

This test program confirmed the design integrity of the engine system and of all the major components in the engine operating environment. It also revealed several areas in which improvements to designs should be made in conjunction with engine development.

PLANNED FUTURE ACTIVITY

The UOME ICTB is currently being prepared for altitude testing at the NASA White Sands Test Facility. A turbine exhaust line, nozzle coolant manifold, and nozzle extension adapter (which allows use of the current OME nozzle) have been fabricated and integrated into the ICTB assembly. Testing is scheduled to be initiated in late summer of 1990.

The objectives of the altitude engine test program include establishing engine performance at simulated altitude conditions, establishing post fire engine purge requirements, determining minimum turbopump interpropellant seal purge requirements, definition of mixture ratio and chamber pressure operating envelope, determining performance effect of high and low temperature propellants, and demonstration of mission duty cycle.

REFERENCES

1. Boyd, W., and Mallini, C. "Shuttle Performance Enhancement Using An Uprated OMS Engine", AIAA/ASME/SAE/ASEE Joint Propulsion Conference, Boston, Massachusetts, July, 1988
2. Boyd, W., "Uprated OMS Engine for Upper Stage Propulsion", JANNAF Propulsion Conference, New Orleans, Louisiana, August, 1986
3. Boyd, W., and Brasher, W. "Uprated OMS Engine Status and Future Applications", AIAA/ASME/SAE/ASEE 22nd Joint Propulsion Conference, Huntsville, Alabama, June, 1986